Songklanakarin J. Sci. Technol.
40 (4), 824-830, Jul - Aug. 2018

http://www.sjst.psu.ac.th

Original Article

Preparation of aluminum doped zinc oxide targets and RF magnetron sputter thin films with various aluminum doping concentrations

Narongchai Boonyopakorn[1, 2*], Ratthapol Rangkupan[3], and Tanakorn Osotchan[4]

[1] *Program of Science, Faculty of Science and Technology, Nakhonpathom Rajabhat University, Mueang, Nakhon Pathom, 73000 Thailand*

[2] *Research Unit of Thin Film Coating in Vacuum, Research and Development Institute, Nakhonpathom Rajabhat University, Mueang, Nakhon Pathom, 73000 Thailand*

[3] *Metallurgy and Materials Science Research Institute, Chulalongkorn University, Pathum Wan, Bangkok, 10330 Thailand*

[4] *Department of Physics, Faculty of Science, Mahidol University, Ratchathewi, Bangkok, 10400 Thailand*

Received: 9 December 2016; Revised: 15 March 2017; Accepted: 29 April 2017

Abstract

In this work, aluminum doped zinc oxide (AZO) ceramic targets were prepared from ZnO powder and Al_2O_3 powder with varying amounts of Al_2O_3 doped in a range of 1-5 wt%. The mixed ZnO and Al_2O_3 powders were pressed at a pressure of 80 MPa into disks and sintered at 1,300 °C for 5 h in air. The crystal structures of the sintered targets were characterized by X-ray diffraction (XRD) technique. It was found that the XRD spectra showed a hexagonal (wurtzite) structure of ZnO for all Al_2O_3 doped films. However, as the amount of Al_2O_3 increased over 2 wt%, the gahnite ($ZnAl_2O_4$) phase could be observed in the XRD spectra. The AZO films were deposited on glass slides at room temperature and post-annealed at 500 °C in a vacuum for 1 h. The film structures, Al/Zn ratio between the Al and Zn atoms, and the electrical properties were characterized. It was found that an increase of Al_2O_3 content in the target gave a higher Al doping concentration in the film which resulted in more Al substitutions in the Zn sites which in turn resulted in an increase of carrier concentration. The crystal structure of the AZO films deposited from undoped and 1 wt% Al_2O_3-doped targets showed the (002) preferred orientation and drastically decreased at higher Al doping concentrations. The mobility of the charge carrier was affected by lower crystallinity due to grain boundary scattering. In addition, the excess Al in the film may play a role as impurity scattering centers. A decrease of Hall mobility resulted in increased resistivity. The minimum resistivity of 2.01×10^{-3} Ω.cm could be achieved for the AZO films deposited from 1 wt% Al_2O_3-doped ZnO targets.

Keywords: AZO films, Al-doping concentration, RF magnetron sputtering

*Corresponding author
Email address: nb_narongk@yahoo.com

1. Introduction

Transparent conducting oxide (TCO) films, such as tin-doped indium oxide (ITO), fluorine-doped tin oxide (FTO) and aluminum-doped zinc oxide (AZO), have been widely used in many applications such as solar cells (Zhao *et al*., 2016), gas sensors (Hosseinnejad *et al*., 2016), and thin film transistors (Navamathavan *et al*., 2008). Among these TCOs, the ITO is the mostly used because of high visible transmission and low electrical resistivity. However, indium is an expensive material, hence there are efforts to prepare other low-cost, good quality, and indium-free TCO films (Zhang *et al*., 2016). The AZO film is especially attractive due to its good electrical properties with high transmission in the visible light region comparable to the ITO. Unique combinations of electrical and optical properties of the TCO films result from good crystalline structure and high carrier concentration with high mobility in the film. The carrier concentration in the AZO film originates from oxygen vacancy and the substitution of Al^{3+} into Zn^{2+} sites of the zinc oxide structure.

There are various deposition techniques used to prepare the AZO films such as spray pyrolysis (Muiva *et al*., 2011), pulse laser deposition (Chen *et al*., 2005), sol-gel (Mamat *et al*., 2010), and radio frequency (RF) magnetron sputtering. In the magnetron sputtering technique, the oxygen vacancy and Al^{3+} substitution are dependent on deposition parameters such as working pressure (Houng *et al*., 2008), sputtering power (Besleaga *et al*., 2014), substrate temperature (Li *et al*., 2009), distance from target to substrate (Jeong *et al*., 2004), and oxygen partial pressure (Yim *et al*., 2006) which have been wildly investigated.

In addition, Al doping concentration is an important parameter that can affect the properties of the AZO films prepared by the sputtering technique (Besleaga *et al*., 2014). In this work, the effects of Al doping concentrations were studied by varying the percentage of Al in AZO sputtering targets. Low-cost zinc oxide (ZnO, 99.7%) and aluminum oxide (Al_2O_3, 99.99%) powders were used as raw materials to prepare the AZO sputtering targets. The properties of the prepared AZO films were then investigated. The AZO films were prepared by RF magnetron sputtering at room temperature and post-annealed at 500 °C in a vacuum.

2. Experimental Details

2.1 Sputtering target preparations and characterizations

The experimental procedure began with preparations of the Al_2O_3-doped ZnO ceramic targets by mixing ZnO powder (99.7%) and Al_2O_3 powder (99.99%) in the weight percent (wt%) ratios of (Al_2O_3/ZnO) 0, 1, 2, 3, 4, and 5 wt%. The mixed powders were milled by a ring-mill machine and pressed into disks with a diameter of 82.2 mm and then sintered at 1,300 °C in air for 3 h. The diameters of the ceramic targets were reduced to about 74.0 mm after sintering. The crystal structures of the AZO targets were characterized using the X-ray diffraction technique (D8 diffractrometer, Bruker). Surface morphologies and composition were analyzed using a scanning electron microscope (SEM) and energy dispersive X-ray (EDX) spectroscopy (SU3500, Hitachi) respectively. Peak intensity in the EDX measurement was determined with ZAF correction using an energy dispersive X-ray microanalyzer (EMAX Energy, Horiba) attached to the SEM (SU3500, Hitachi). In addition, the accuracy of elemental assignment and peak position was confirmed using a commercial 2 wt% Al_2O_3-doped ZnO ceramic target (Kurt J. Lesker) as an internal reference to confirm peak position with which the atomic percentage (at.%) of the target compositions were investigated.

2.2 AZO film preparations and characterizations

For preparations of AZO films, glass slides (size 2.5x2.5 cm) were used as the substrates. They were ultrasonically cleaned by steeping the substrates in acetone and ethyl-alcohol respectively for 10 min each and blowing dry with nitrogen gas before placing them into a vacuum chamber. The AZO films were prepared in a home-built sputtering system at room temperature. Before the sputtering process, the vacuum chamber was evacuated to a background pressure of about $1.0x10^{-5}$ mbar by rotary and diffusion pumps. High-purity argon gas (99.995%) was then filled into the chamber and the working pressure was maintained at $5.0x10^{-3}$ mbar. RF power was maintained at 100 W for all depositions at a frequency of 13.56 MHz (Cito 1310, Comet).

The target was pre-sputtered for 5 min before film deposition. The deposition times were calibrated for a film thickness of 300 nm for 30-45 min. The film thicknesses were also determined by cross-section SEM images of the deposited film/glass substrate. The deposited films were then annealed in vacuum at 500 °C for 1 h. The crystal structure and the electrical properties of the annealed films were characterized using the X-ray diffraction technique (D8 diffractrometer, Bruker) and Hall measurement (HMS-3000, Ecopia), respectively. In addition, atomic percentage (at.%) of Al composition in the film structure was investigated by EDX spectroscopy (SU3500, Hitachi).

3. Results and Discussion

3.1 Crystal structure of prepared AZO targets

The XRD patterns of the ZnO and 1-5 wt% of Al_2O_3-doped ZnO ceramic targets sintered at 1,300 °C for 3 h were collected (Figure 1). The XRD spectra of ZnO and 1-2 wt% Al_2O_3-doped ZnO ceramic targets show the hexagonal (wurtzite) structure of the ZnO (ICDD: 01-089-0510). The peak positions remained unchanged with the increase in the wt% of Al_2O_3 doped in the ZnO structure. However, it can be noticed that peaks of gahnite ($ZnAl_2O_4$) phase (ICDD: 01-070-8181) could be observed with the increase in the wt% of Al_2O_3 doped in the target higher than 2 wt%. This implied residual Al_2O_3 which could form the gahnite phase. Therefore, in high wt% Al_2O_3 doped ZnO, not all Al atoms substituted into the Zn sites of the AZO crystal structure. This result was consistent with that reported by Besleaga *et al*. (2014) in which the gahnite phase could be detected for the AZO sputtering targets doped with 2.2 wt% Al_2O_3.

In order to analyze the gahnite phase that appeared in the XRD spectra, backscattered electron (BSE) images and the characteristic X-ray mapping of the elements were performed. Figure 2(a) shows the BSE image of the surface morphology for the 5 wt% Al_2O_3-doped ZnO ceramic target. It can be

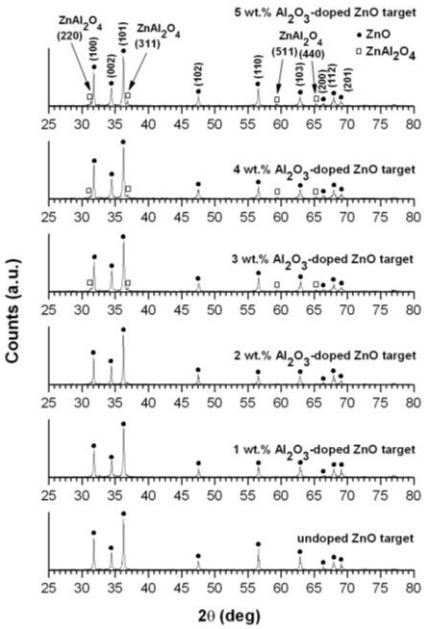

Figure 1. XRD pattern of AZO ceramic target doped with Al_2O_3 from 0-5 wt%.

obviously seen that there were two distinguishable areas such as white and black areas. The BSE image was performed by secondary electrons scattered from the incident object. If the incident object is composed of various elements or morphology, then the scattered electrons will be different. Consequently, the image will show different colors corresponding to the scattered electrons as gray to white for high scattering and dark-gray to black for the scattering of lighter electrons. In order to specify the elements in these two areas, characteristic X-ray mapping was performed (Figure 2(b)-(e). The images of element distribution were performed by the characteristic X-ray emitted from each element from the primary incident electrons. Therefore, from Figure 2, the amounts of Al and O in the black area can be seen. In Figures 2(b) and (d), is higher than that in the white area. On the other hand, the amount of Zn is higher in the white area than that in the black area as shown in the Figure 2(c). The atomic ratio of Zn:Al:O for $ZnAl_2O_4$ is 1:2:4 while the Al substitution in the Zn position in the film structure was one by one. Thus, the $ZnAl_2O_4$ phase needs more Al and O atoms than in the case of Al substitutions. Therefore, the black area represented the gahnite ($ZnAl_2O_4$) phase in the target which results in the peaks of gahnite phase in the XRD spectra (Figure 1). The compositions in the black and white areas were confirmed by the EDX

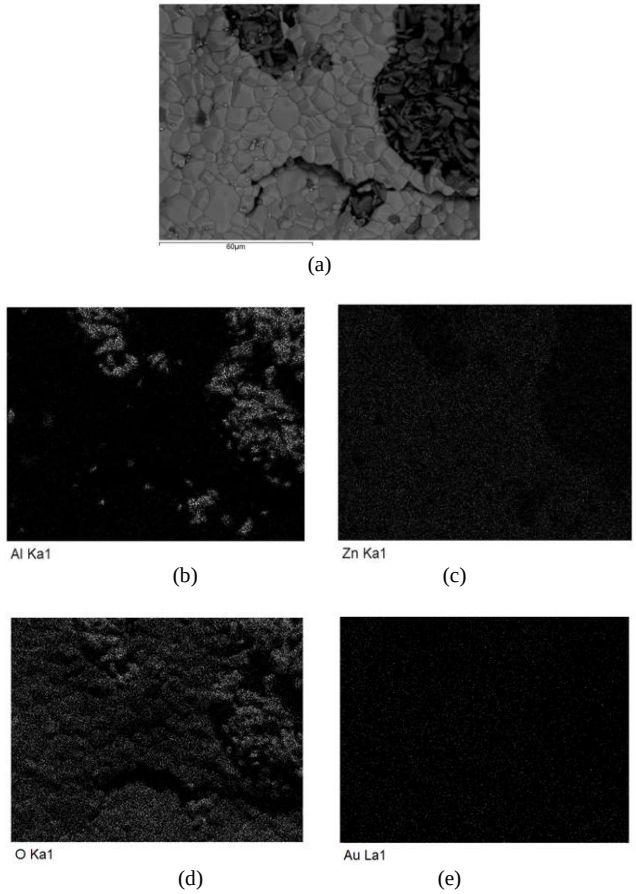

Figure 2. Surface morphology of 5 wt% Al_2O_3-doped ZnO ceramic target (a) backscattered electron (BSE) image and characteristic X-ray mappings for element distributions of (b) Al, (c) Zn, (d) O and (e) Au.

spectroscopic images which represents the wt% of each composition in both areas (Figure 3). In addition, the wt% and at.% of Zn, Al, and O are shown in the inset tables. It can be seen that the atomic ratio of Zn:Al:O is 1:1.67:4.37 which is very close to that of the atomic ratio of the $ZnAl_2O_4$ molecule as discussed above. Moreover, Au film was coated on the specimen surface before the SEM. Therefore, the X-ray mapping of the Au element, as shown in Figure 2(e), showed a uniform distribution on the specimen surface which implied uniform coating of the Au film.

3.2 Crystal structure of deposited AZO films

The XRD spectra of the AZO films deposited from the undoped and 1-5 wt% Al_2O_3-doped ZnO targets were studied (Figure 4). The films deposited from undoped and 1 wt% of Al_2O_3-doped ZnO targets indicated the preferred orientation in (002) plane at $2\theta \approx 34.54°$ and 34.74°, respectively. The 2θ value of the film deposited from the undoped ZnO target was very close to the standard value of 34.45° of the ZnO crystal structure. For the AZO films deposited from 1 wt% Al_2O_3-doped ZnO target, the 2θ value shifted to a higher angle which may be attributed to different ionic radii of Zn^{2+} and Al^{3+} being 72 and 53 pm, respectively. Therefore, the Al substitution in the Zn sites of the film structure can bring about a shorter length of the *c*-axis. However, for film with a higher wt% of Al_2O_3 doping concentration, the (002) peak drastically decreased and disappeared for the AZO film prepared from 5 %wt. For film with Al_2O_3 doped, the low intensities (100) and (101) peaks were observed. However, there are no $ZnAl_2O_4$ peaks detected in any of deposited films which may imply that the Al atoms were substituted in the ZnO sites or segregated to the grain boundary in the film structure.

The decrease in the (002) peak as the wt% of Al-doped in ZnO structure increased may be due to the difference in ion size between Zn^{2+} and Al^{3+} which created stress in the film structures. Appearance of the stress resulted in the loss of periodic arrangement, random orientations and, consequently, poor crystallinity in the film structures as discussed by Muiva *et al*. (2011), which reported AZO films prepared by spray pyrolysis technique at substrate temperature of 420 °C with different atomic percent (at.%) from 0-10 at.%.

3.3 Al composition and electrical properties of deposited AZO films

The percentage amounts of Al doping concentration in the AZO films structure were confirmed by EDX results for the films deposited from 0 to 5 wt% of Al_2O_3 doped in the AZO targets (Figure 5). From linear regression, the atomic percentage of Al increased linearly with weight percentage of Al_2O_3-doped in the target. The atomic percentage of Al doping concentration increased from 3.45 to 12.77 at.% in the AZO film deposited by the targets as the wt% of Al_2O_3 doping increased from 1 to 5 wt%. The higher at.% of Al doping concentrations was consistent with an increase of the carrier concentration in the AZO films which increased from 3.40×10^{19} cm^{-3} for undoped ZnO film to 9.67×10^{20} cm^{-3} for 4 wt% Al_2O_3 doped film (Figure 6). The higher carrier concentration in Al-doped ZnO film resulted from Al substitutions in Zn sites in the film structure. Therefore, as the Al doping amount increased, there was an increase in Al substitution in the film structure and higher carrier concentration. However, as the Al_2O_3 doping concentration increased to 5 wt%, the carrier concentration reduced to 6.86×10^{20} cm^{-3}. The excess Al atoms in the film structure had no longer contributed to the Al substitutions but played a role as electron traps resulting in reducing the carrier concentration. This result was consistent with that reported by El Manounia *et al*. (2006).

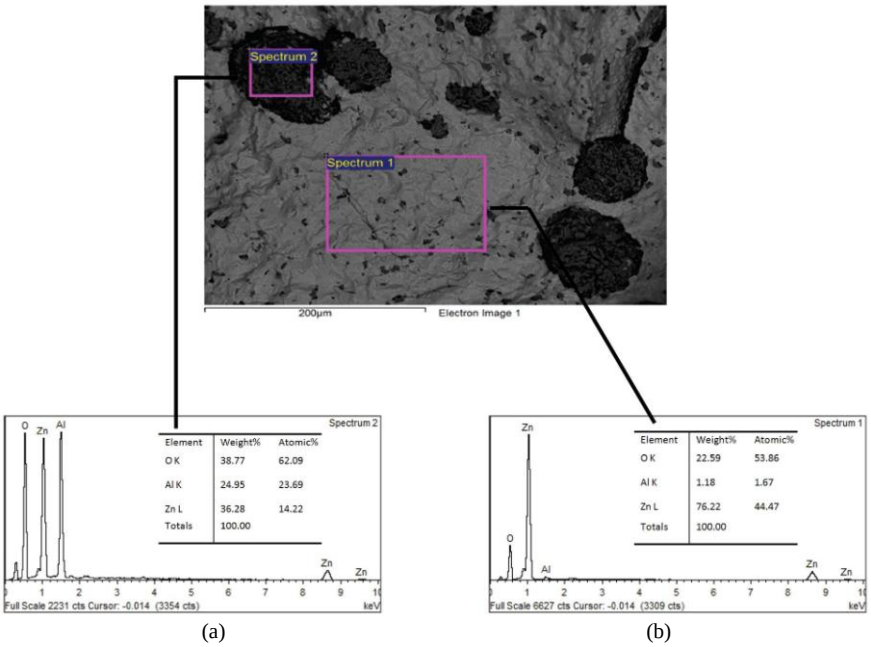

(a) (b)

Figure 3. EDX measurements of sanded 5 wt% Al_2O_3-doped ZnO target in the white and black areas.

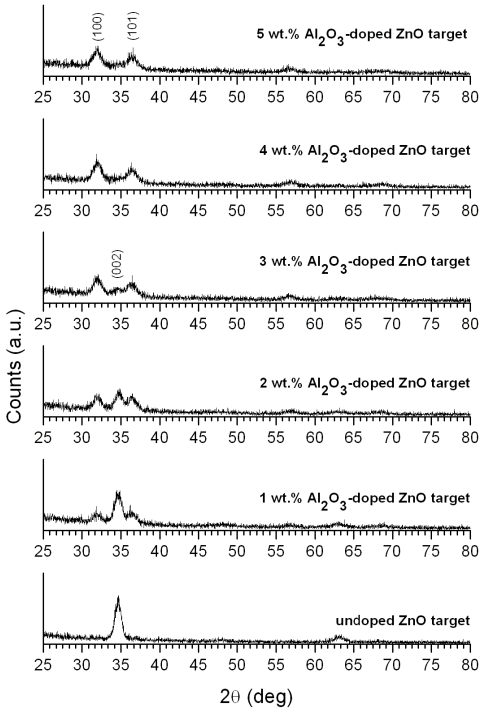

Figure 4. XRD spectra of AZO films deposited from prepared ceramic target doped with Al_2O_3 from 0-5 wt%.

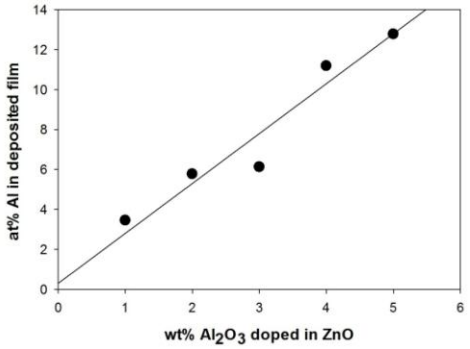

Figure 5. Al atomic percentage of AZO films deposited from prepared ceramic target doped with Al_2O_3 from 0-5 wt% extracted from EDX results.

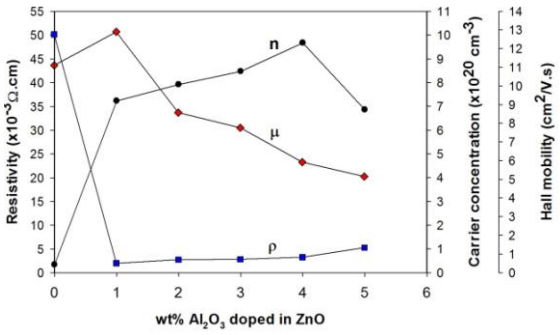

Figure 6. Electrical properties of AZO films deposited from prepared ceramic target doped with Al_2O_3 from 0-5 wt%.

In addition, the excess Al atoms doped in the crystalline structure may segregate in the grain boundary or interstitial sites and act as impurity scattering centers which can reduce mobility of the carriers. Moreover, according to the XRD spectra (Figure 2), the decrease in the Hall mobility may be due to grain boundary scattering because of lattice distortion in the film structure with high Al_2O_3-doping concentration as reported by Zhao *et al*. (2016).

The electrical resistivity is inversely proportional to the carrier concentration and the mobility according to $1/\rho = ne\mu$, where e is the electron charge. For undoped ZnO film, the resistivity was as high as 5.02×10^{-2} Ω.cm due to the very low carrier concentration of 3.40×10^{19} cm^{-3}. Then the resistivity drastically dropped to 2.01×10^{-3} Ω.cm due to the increased carrier concentration. For the AZO films deposited from 1-4 wt% Al_2O_3 doped ZnO targets, the carrier concentration increased with higher Al doping concentration while the mobility became smaller. This resulted in increased resistivity from 2.01×10^{-3} Ω.cm to 9.67×10^{-3} Ω.cm. It can be noticed that the mobility had a much greater effect than the carrier concentration. Therefore, in order to achieve lower electrical resistivity of the AZO film, it is necessary to improve the mobility by increasing the crystallinity of the film structure.

4. Conclusions

In this research, AZO targets were prepared from ZnO powder and Al_2O_3 powder as 0-5 wt% Al_2O_3-doped. The sintering temperature was set at 1300 °C for 3 h in air. It was found that the gahnite ($ZnAl_2O_4$) phase appeared in XRD spectra of the sintered targets. After that AZO films were deposited from the sintered AZO targets by the RF magnetron sputtering technique. The deposited films were then annealed at 500 °C in vacuum for 1 h. It was found that the amount of Al in the film increased as the wt% of Al_2O_3 doping increased in the target.

The crystal structure and electrical properties of the films were affected by the concentration of Al doping in the film structures. Higher Al doping concentrations resulted in poor crystallinities and an increase in the carrier concentration. However, poor crystallinities can cause grain boundary scattering to be dominant which then contributed to low Hall mobility. In addition, for films from the 5 wt% Al_2O_3 doped target, the excess Al atoms in the film played the role as electron traps leading to a decrease in the carrier concentration.

It can be concluded that high quality AZO films deposited by the RF magnetron sputtering technique can be achieved from prepared AZO targets with the appropriate wt% of Al_2O_3-doped target.

Acknowledgements

The authors would like to thank Asst. Prof. Ratthapol Rangkupan, Metallurgy and Materials Research Institute Chulalongkorn University, for his kindness for the SEM and EDX measurements. The authors also would like to thank the Research and Development Institute, Nakhonpathom Rajabhat University for the research funding.

References

Agashe, C., Kluth, O., Schöpe, G., Siekmann, H., Hüpkes, J., & Rech, B. (2003). Optimization of the electrical properties of magnetron sputtered aluminum-doped zinc oxide films for opto-electronic applications. *Thin Solid Films, 442*, 167-172.

Ayadi, Z. B., El Mir, L., Djessas, K., & Alaya, S. (2009). Effect of the annealing temperature on transparency and conductivity of ZnO:Al thin films. *Thin Solid Flims, 517*, 6305-6309.

Ayadi, Z. B., Mahdhi, H., Djessas, K., Gauffier, L. L., El Mir, L., & Alaya, S. (2014). Sputtered Al-doped ZnO transparent conducting thin films suitable for silicon solar cells. *Thin Solid Flims, 553*, 123-126.

Besleaga, C., Ion, L., & Antohe, S. (2014). AZO Thin films synthesized by RF-magnetron sputtering: The role of deposition power. *Romanian Reports in Physics, 66*, 993-1001.

Chang, J. F., & Hon, M. H. (2001). The effect of deposition temperature on the properties of Al-doped zinc oxide thin films. *Thin Solid Films, 386*, 79-86.

Chen, X., Guan, W., Fang, G., & Zhao, X. Z. (2005). Influence of substrate temperature and post-treatment on the properties of ZnO:Al thin films prepared by pulsed laser deposition. *Applied Surace Science, 252*, 1561-1567.

El Manounia, A., Manjón, F. J., Mollar, M., Marí, B., Gómez, R., López, M. C., &Ramos-Barrado, J. R. (2006). Effect of aluminium doping on zinc oxide thin films grown by spray pyrolysis. *Superlattices and Microstructures, 39*, 185–192.

El Manounia, A., Manjón, F. J., Perales, M., Mollar, M., Marí, B., López, M. C., & Ramos-Barrado, J. R. (2007). Effect of thermal annealing on ZnO:Al thin films grown by spray pyrolysis. *Superlattices and Microstructures, 42*, 134–139.

Hosseinnejad, M. T., Ghoranneviss, M., Hantehzadeh, M. R., & Darabi, E. (2016). Characterization and hydrogen gas sensing performance of Al-doped ZnO thin films synthesized by low energy plasma focus device. *Journal of Alloys and Compounds, 689*, 740–750.

Houng, B., His, C. S., Hou, B. Y., & Fu, S. L. (2008). Effect of process parameters on the growth and properties of impurity-doped zinc oxide transparent conducting thin films by RF magnetron sputtering. *Vacuum, 83*, 534-539.

Jeong, S. H., & Boo, J. H. (2004). Influence of target-to-substrate distance on the properties of AZO films grown by RF magnetron sputtering. *Thin Solid Films, 447-448*, 105-110.

Jeong, S. H., Kho, S., Jung, D., Lee, S. B., & Boo, J. H. (2003). Deposition of aluminum-doped zinc oxide films by RF magnetron sputtering and study of their surface characteristics. *Surface and Coatings Technology, 174-175*, 187-192.

Jeong, S. H., Lee, J. W., Lee, S. B., & Boo, J. H. (2003). Deposition of aluminum-doped zincoxide films by RF magnetron sputtering and study of their structural, electrical and optical properties. *Thin Solid Films, 435*, 78-82.

Kuo, S. Y., Chen, W. C., Lai, F.-I., Cheng C. P., Kuo, H. C., Wang, S. C., & Hsieh, W. F. (2006). Effects of doping concentration and annealing temperature on properties of highly-oriented Al-doped ZnO films. *Journal of Crystal Growth, 287*, 78-84.

Lee, J. H., & Park, B. O. (2004). Characteristics of Al-doped ZnO thin films obtained by ultrasonic spray pyrolysis: effects of Al doping and an annealing treatment. *Materials Science and Engineering B, 106*, 242–245.

Li, X. Y., Li, H. J., Wang, Z. J., Xia, H., Xiong, Z. Y., Wang, J. X., & Yang, B. C. (2009). Effect of substrate temperature on the structural and optical properties of ZnO and Al-doped ZnO thin films prepared by dc magnetron sputtering. *Optics Communications, 282*, 247-252.

Mamat, M. H., Sahdan, M. Z., Khusaimi, Z., Ahmed, A. Z., Abdullah, S., & Rusop, M. (2010). Influence of doping concentrations on the aluminum doped zinc oxide thin films properties for ultraviolet photoconductive sensor applications. *Optical Materials, 32*, 696-699.

Muiva, C. M., Sathiaraj, T. S., & Maabong, K. (2011). Effect of doping concentration on the properties of aluminium doped zinc oxide thin films prepared by spray pyrolysis for transparent electrode applications. *Ceramics International, 37*, 555-560.

Navamathavan, R., Choi, C. K., Yang, E. J., Lim, J. H., Hwang, D. K., & Park, S. J. (2008). Fabrication and characterizations of ZnO thin film transistors prepared by using radio frequency magnetron sputtering. *Solid-State Electronics, 52*, 813-816.

Roth, A. P., Webb, J. B., & Williams, D. F. (1982). Band-gap narrowing in heavily defect-doped ZnO. *Physical Review B, 25*(12), 7836-7839.

Shelke, V., Sonawane, B. K., Bhole, M. P., & Patil, D. S. (2009). Effect of annealing temperature on the optical and electrical properties of aluminum doped ZnO films. *Journal of Non-Crystalline Solids, 355*, 840-843.

Shishiyanu, S. T., Shishiyanu, T. S., & Lupan, O. I. (2005). Sensing characteristics of tin-doped ZnO thin films as NO_2 gas sensor. *Sensors and Actuators B, 107*, 379-386.

Singh, A. V., Kumar, M., Mehra, R. M., Wakahara, A., & Yoshida, A. (2001). Al-doped zinc oxide (ZnO:Al) thin films by pulsed laser ablation. *Journal of the Indian Institute of Science, 81*, 527-533.

Suchea, M., Christoulakis, S., Katsarakis, N., Kitsopoulos, T., & Kiriakidis, G. (2007). Comparative study of zinc oxide and aluminum doped zinc oxide transparent thin films grown by direct current magnetron sputtering. *Thin Solid Films, 515*, 6562-6566.

Yim, K., & Lee, C. (2006). Optical properties of Al-doped ZnO thin films deposited by two different sputtering methods. *Crystal Research and Technology, 41*, 1198–1202.

Zhang, Z., Tang, Y., Chen, J., & Chen, J. (2016). Influence of low sputtering pressure on structural, electrical and optical properties of Al-doped zinc oxide thin films. *Physica B, 495*, 76-81.

Zhao, X., Shen, H., Zhou, C., Lin, S., Li, X., Zhao, X., . . . Lin, H. (2016). Preparation of aluminumdoped zinc oxide films with low resistivity and outstanding transparency by a sol–gel method for potential applications in perovskite solar cell. *Thin Solid Films*, *605*, 208-214.